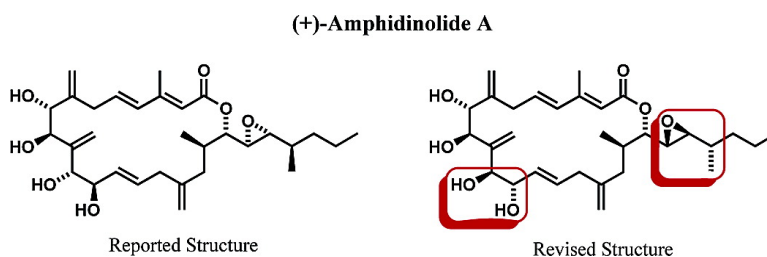


## Total Synthesis of (+)-Amphidinolide A. Structure Elucidation and Completion of the Synthesis

Barry M. Trost, Paul E. Harrington, John D. Chisholm, and Stephen T. Wroblewski

*J. Am. Chem. Soc.*, **2005**, 127 (39), 13598-13610 • DOI: 10.1021/ja053365y • Publication Date (Web): 07 September 2005

Downloaded from <http://pubs.acs.org> on March 25, 2009



### More About This Article

Additional resources and features associated with this article are available within the HTML version:

- Supporting Information
- Links to the 13 articles that cite this article, as of the time of this article download
- Access to high resolution figures
- Links to articles and content related to this article
- Copyright permission to reproduce figures and/or text from this article

[View the Full Text HTML](#)

## Total Synthesis of (+)-Amphidinolide A. Structure Elucidation and Completion of the Synthesis

Barry M. Trost,\* Paul E. Harrington, John D. Chisholm, and Stephen T. Wroblewski

Contribution from the Department of Chemistry, Stanford University,  
Stanford, California 94305-5080

Received May 23, 2005; E-mail: bmtrost@stanford.edu

**Abstract:** The structure elucidation of (+)-amphidinolide A, a cytotoxic macrolide, has been accomplished by employing a combination of NMR chemical shift analysis and total synthesis. The 20-membered ring of amphidinolide A was formed by a ruthenium-catalyzed alkene–alkyne coupling to forge the C15–C16 bond. Using the reported structure **1** as a starting point, a number of diastereomers of amphidinolide A were prepared. Deviations of the chemical shift of key protons in each isomer relative to the natural material were used as a guide to determine the locations of the errors in the relative stereochemistry. The spectroscopic data for the synthetic and natural material are in excellent agreement.

### Introduction

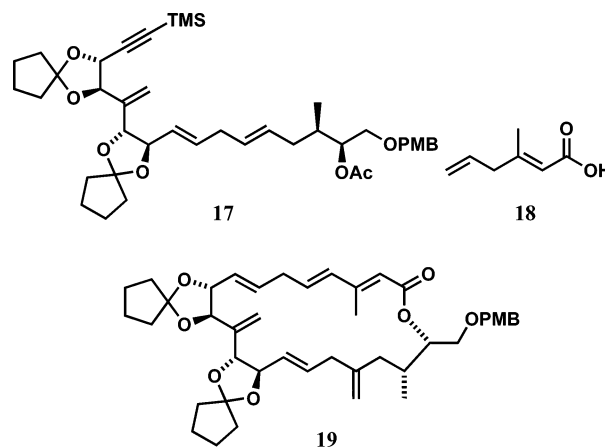
In the previous paper in this issue,<sup>1</sup> three strategies were outlined for the synthesis of **1** (Figure 1). Either **2**, **3**, or **4** could potentially serve as a precursor to **1**. Once a reliable route to **1** is developed, the door is open to allow access to diastereomers of **1**, with the ultimate goal being the determination of the structure of amphidinolide A and confirmation by synthesis. However, before this can begin, one or more of the routes shown in Figure 1 must be established.

### Results and Discussion

**Macrocyclization at C6–C7.** The first approach to the proposed structure of amphidinolide A (**1**) was via an intermolecular ruthenium-catalyzed alkene–alkyne coupling to form the C15–C16 bond followed by the intramolecular coupling to form the C6–C7 bond. As shown in Scheme 1, [CpRu(MeCN)<sub>3</sub>]-PF<sub>6</sub>-catalyzed alkene–alkyne coupling of **10** with (trimethylsilyl)alkyne **11** effected coupling. In DMF, the reaction proceeded slowly, giving only a 34% yield [96% based upon recovered starting material (brsm)] but in a gratifying 9:1 branched (**12**) to linear (**17**) regioselectivity with respect to the alkyne. In acetone, the conversion improved (76% yield, 91% brsm), but the regioselectivity decreased to 4:1. Adding 5 vol % DMF to acetone restored the regioselectivity but at some expense of conversion (48–66% yield, ~96% brsm).

Diene **12** was converted to **13** with barium hydroxide in methanol. Under these conditions, the alkyne in **12** was also deprotected. The direct esterification of **13** with **18** proved to be problematic. Esterification with DCC/DMAP resulted in complete isomerization of the base-sensitive 1,4-diene in **18** to

give the fully conjugated 1,3-diene. Attempts to suppress this isomerization by using HOBt as an additive<sup>2</sup> or by converting **18** to the corresponding acid chloride were also unsuccessful. The use of tributylphosphine as a nonbasic acylation catalyst<sup>3</sup> in place of DMAP gave similar results. To circumvent this problem, alcohol **13** was esterified with 2-butynoic acid to yield **14** in 57% yield. Conjugate addition of allyl copper at –78 °C to **14** afforded the desired macrocyclization substrate **15** in 55% yield.



The initial attempts to form the 20-membered ring employed [CpRu(MeCN)<sub>3</sub>]-PF<sub>6</sub>. However, exposure of a 0.05 M solution of **15** in DMF at room temperature to 10 mol % [CpRu(MeCN)<sub>3</sub>]-PF<sub>6</sub> afforded trace amounts of unidentified byproducts along with significant amounts of recovered **15**. Although the byproducts were not rigorously characterized, their <sup>1</sup>H NMR spectra

(1) Trost, B. M.; Wroblewski, S. T.; Chisholm, J. D.; Harrington, P. E.; Jung, M. *J. Am. Chem. Soc.* **2005**, *127*, 13589.

(2) Trost, B. M.; Belletire, J. L.; Godleski, S.; McDougal, P. G.; Balkovec, J. *M. J. Org. Chem.* **1986**, *51*, 2370.

(3) Vedejs, E.; Bennett, N. S.; Conn, L. M.; Diver, S. T.; Gingras, M.; Lin, S.; Oliver, P. A.; Peterson, M. J. *J. Org. Chem.* **1993**, *58*, 7286.

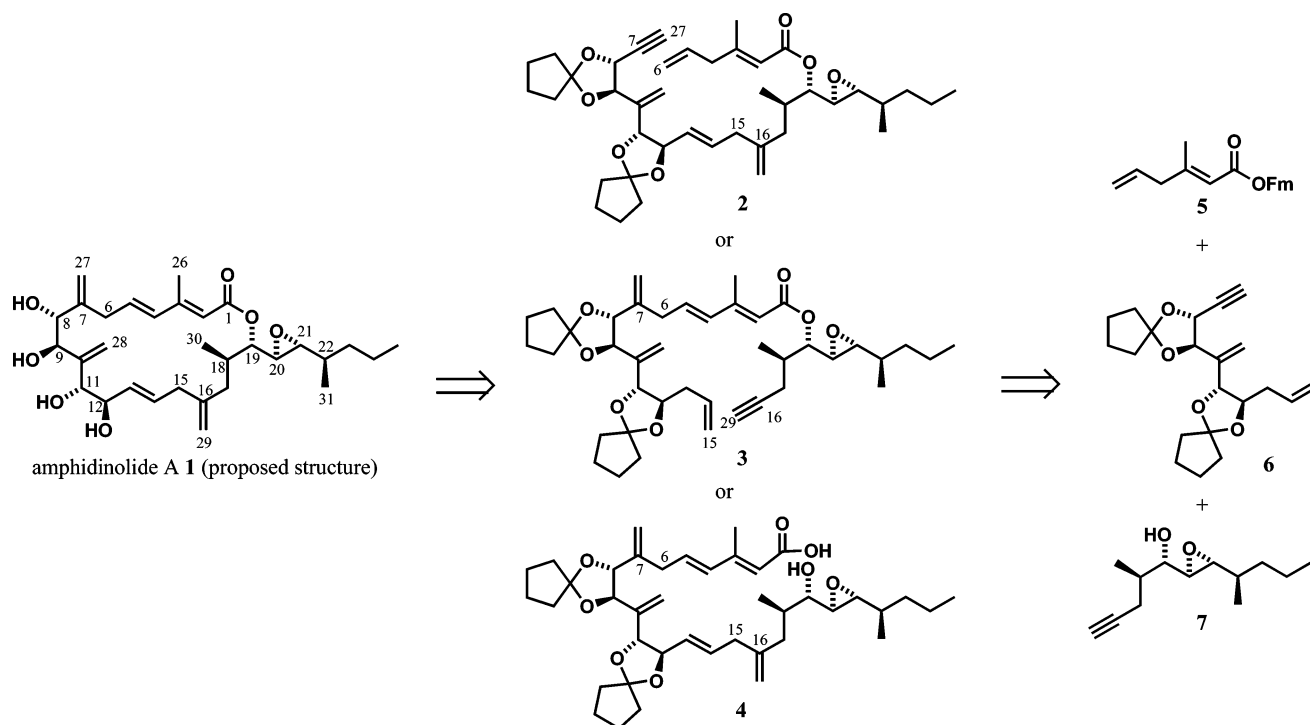


**Figure 1.** Retrosynthetic analysis of amphidinolide A.

were not consistent with **16**. Further examination suggested that the byproducts may have been derived from linear isomer **19** rather than the desired branched isomer **16**. Variation of the catalyst, temperature, and solvent yielded similar results. Formation of the linear isomer over the desired branched isomer was not completely unexpected at this point since previous results from our laboratories have shown that propargylic ethers tend to favor the linear products in *intermolecular* addition reactions under similar conditions.<sup>4a</sup> We were hoping that reaction through a conformationally restricted macrocyclization cycloisomerization might offset the propensity to form the linear products, thereby giving the desired branched isomer.

In another attempt at macrocyclization at C6–C7, the cyclopentylidene protecting groups in **15** were removed by treatment with catalytic CSA in aqueous methanol (Scheme 2). Exposure of **20** to  $[\text{CpRu}(\text{MeCN})_3]\text{PF}_6$  in anhydrous DMF at room temperature gave none of the desired macrocycle **21**, and only unreacted **20** was recovered from the reaction.

**Macrolactonization.** With the inability to form the macrocycle at the C6–C7 bond, a macrolactonization approach was undertaken. Since this approach required an intermolecular addition reaction to form the C6–C7 bond, the model substrates **22–24** were utilized to identify the optimal conditions for this key coupling step (Table 1). This optimization was especially relevant after the failure to convert **15** to **16**.

Coupling of the TMS-protected alkyne **22** was initially investigated since prior work from our laboratories have shown that TMS-protected propargylic ethers tend to favor branched products over linear products in intermolecular additions.<sup>4b</sup> As predicted, exposure of a solution of **22** and **24** to 10 mol %

$[\text{CpRu}(\text{MeCN})_3]\text{PF}_6$  in DMF provided branched isomer **25** with excellent selectivity over linear isomer **27** (Table 1, entry 1). However, the yield of **25** was low possibly due to complexation of the diene product with the active catalyst. To circumvent this issue, terminal alkyne **23** was examined. Alkyne **23** should be more reactive than **22**, but may favor the undesired linear isomer **28**. With  $[\text{CpRu}(\text{MeCN})_3]\text{PF}_6$  as the catalyst, **23** coupled with **24** to provide an acceptable combined yield of **26** and **28**; however, the product ratio favored linear isomer **28** in either acetone or DMF (entries 3 and 4). A literature report suggested that the  $[\text{Cp}^*\text{Ru}(\text{MeCN})_3]\text{PF}_6$ <sup>5</sup> catalyst may improve turnovers in reactions where dienes are the products due to the reduced likelihood of the more sterically demanding catalyst to undergo product inhibition.<sup>6</sup> In the event, an excellent combined yield of **26** and **28** was isolated employing 10 mol %  $[\text{Cp}^*\text{Ru}(\text{MeCN})_3]\text{PF}_6$  in DMF (entry 5). In less polar solvents, the product ratio favored branched isomer **26** (entries 6–8), thus overriding the preference usually observed for propargylic ethers.

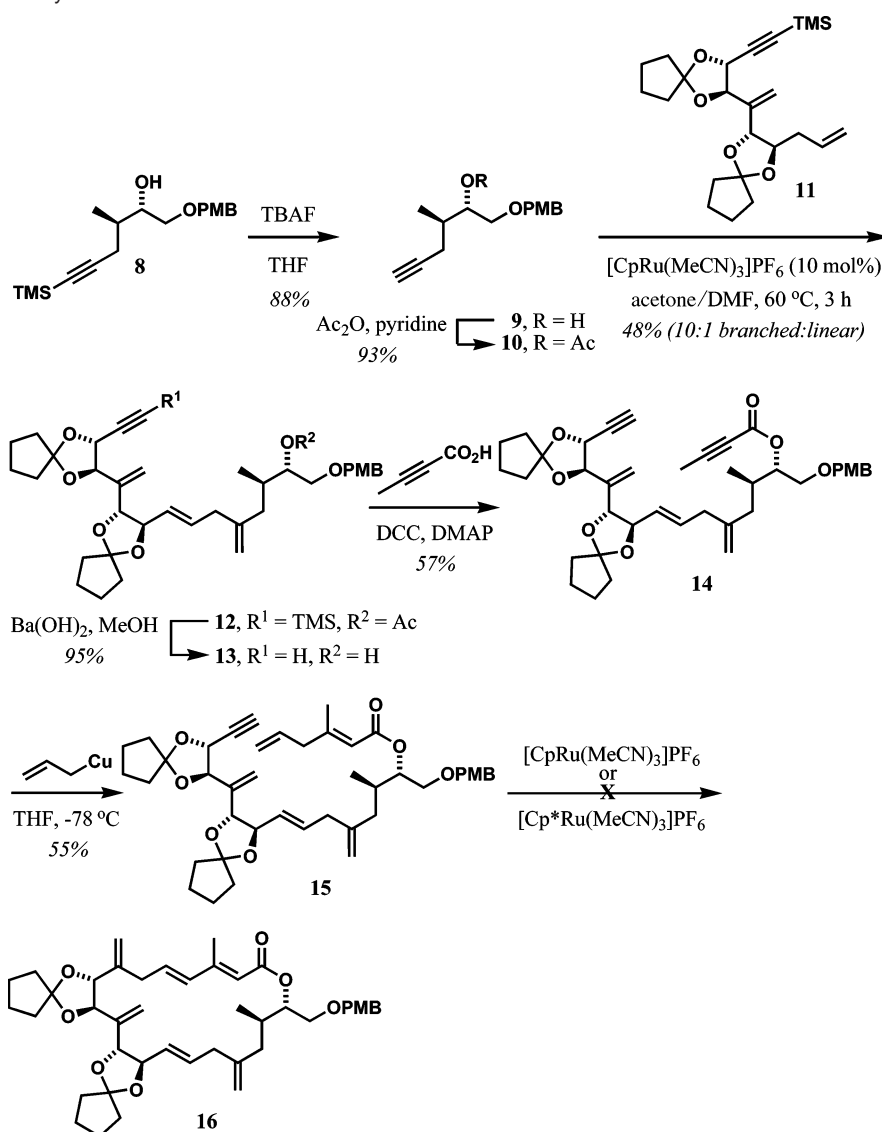
Application of the optimal conditions shown in entry 6 to **29** yielded branched isomer **30** in 53% yield as a 3:1 mixture of branched and linear isomers along with 22% recovered alkyne **29** and 63% recovered alkene **24** (Scheme 3). Hydrolysis of the ethyl ester and acetate in **30** was the next challenge. The sensitivity of the C1–C5 diene to basic conditions has already been described and was a concern here. In the event, exposure of **30** to NaOH in methanol resulted in considerable isomerization of the C1–C5 diene. However, after an extensive screen of conditions, a 47% yield of **31** was realized by treatment of **30** with  $\text{Ba}(\text{OH})_2$  in dioxane/water.

(4) (a) Trost, B. M.; Indolese, A. F.; Mueller, T. J. J.; Treptow, B. *J. Am. Chem. Soc.* **1995**, *117*, 615. (b) Trost, B. M.; Machacek, M.; Schnaderbeck, M. *J. Org. Lett.* **2000**, *2*, 1761.

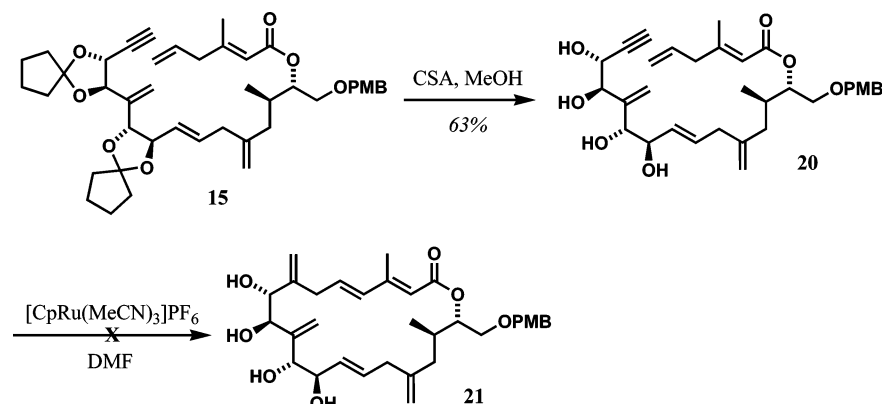
(5) Steinmütz, B.; Schenk, W. A. *Organometallics* **1999**, *18*, 943.

(6) Yamamoto, Y.; Kitahara, H.; Ogawa, R.; Itoh, K. *J. Org. Chem.* **1998**, *63*, 9610.

Scheme 1. Route to Macrocyclization Substrate 15



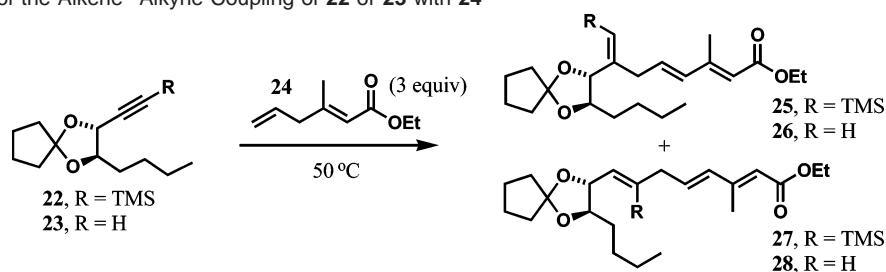
Scheme 2. Attempted Macrocyclization of Free Tetrol 20



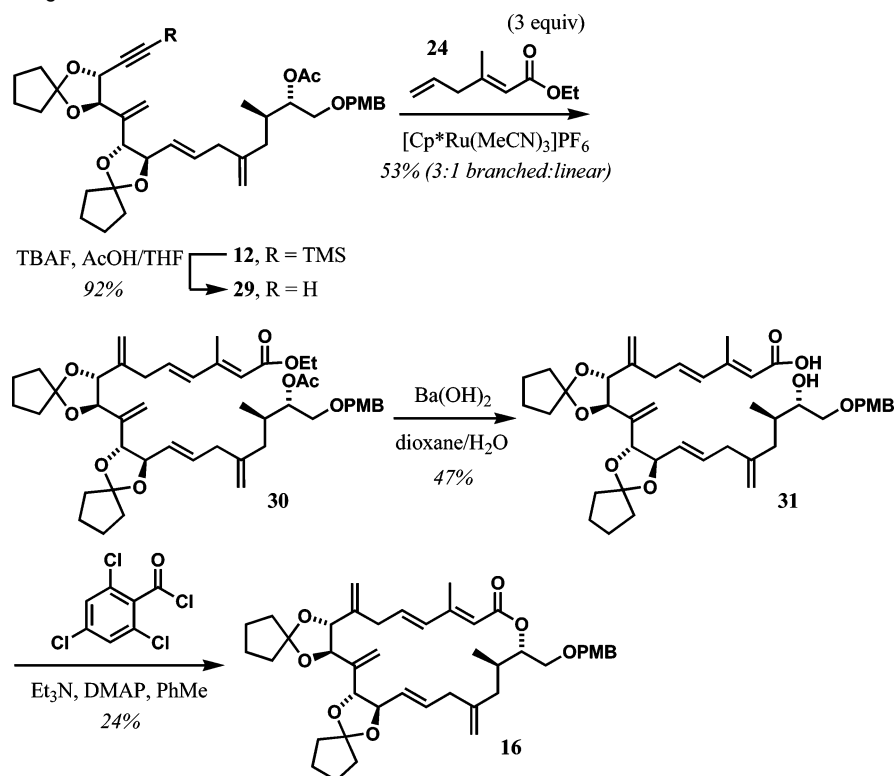
Cyclization of **31** under the Yamaguchi conditions<sup>7</sup> also proved problematic due to the sensitive 1,4-diene in **31**. Under the standard Yamaguchi conditions, extensive isomerization of the unsaturated C1–C5 portion occurred, providing a number of byproducts in addition to a 24% yield of **16**. Therefore, an

improved method for formation of the lactone, without isomerization of the base-sensitive diene, was sought. A number of lactonization methods are available; however, each requires either high temperatures and/or the presence of a base. In an effort to circumvent these limitations, a new macrolactonization protocol was developed based upon the work of Kita.<sup>8</sup> Under these conditions, a carboxylic acid is converted to the corre-

(7) Inanaga, J.; Hirata, H.; Saeki, H.; Katsuki, T.; Yamaguchi, M. *Bull. Chem. Soc. Jpn.* **1979**, *52*, 1989.

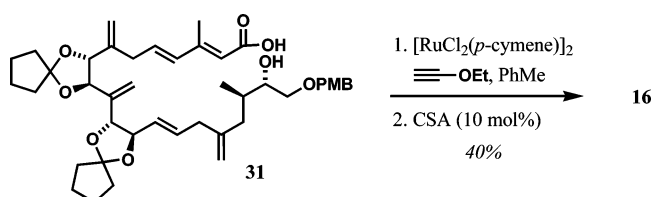
**Table 1.** Optimization of the Alkene–Alkyne Coupling of **22** or **23** with **24**

entry	R	catalyst (10 mol %)	solvent	25:27 or 26:28	yield of 25 + 27 or 26 + 28 (%)
1	TMS	[CpRu(MeCN) <sub>3</sub> ]PF <sub>6</sub>	DMF	>20:1	24
2	TMS	[CpRu(MeCN) <sub>3</sub> ]PF <sub>6</sub>	acetone	>20:1	20
3	H	[CpRu(MeCN) <sub>3</sub> ]PF <sub>6</sub>	DMF	1:1.7	48
4	H	[CpRu(MeCN) <sub>3</sub> ]PF <sub>6</sub>	acetone	1:1.4	40
5	H	[Cp* <i>Ru</i> (MeCN) <sub>3</sub> ]PF <sub>6</sub>	DMF	1:1.2	84
6	H	[Cp* <i>Ru</i> (MeCN) <sub>3</sub> ]PF <sub>6</sub>	acetone	2.3:1	72
7	H	[Cp* <i>Ru</i> (MeCN) <sub>3</sub> ]PF <sub>6</sub>	DCE	2.5:1	55
8	H	[Cp* <i>Ru</i> (MeCN) <sub>3</sub> ]PF <sub>6</sub>	THF	2.8:1	33

**Scheme 3.** Route to Yamaguchi Macrolactonization Substrate **31**

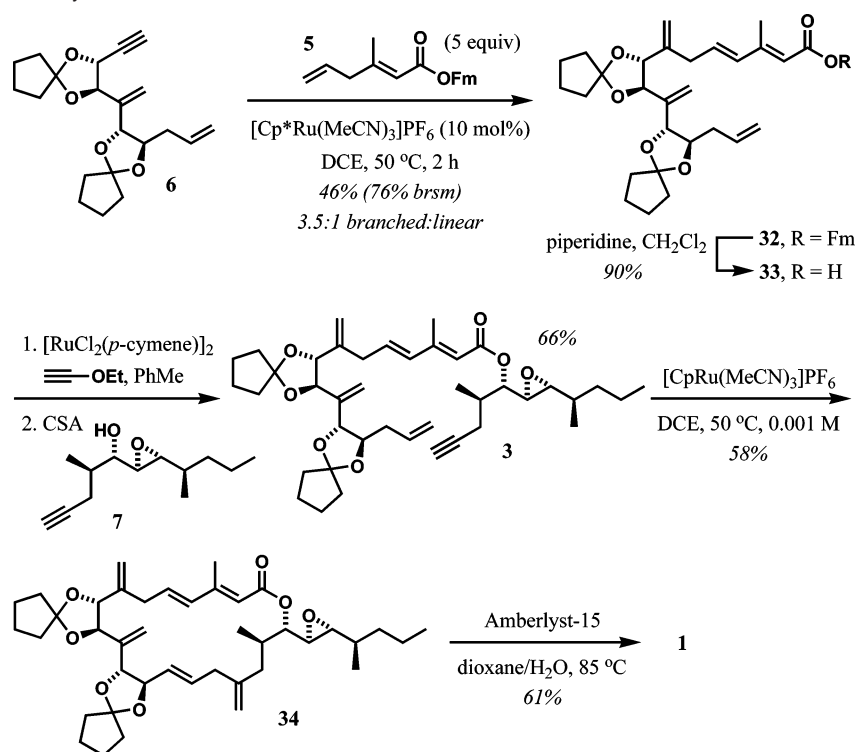
sponding ethoxyvinyl ester with ethyl ethynyl ether and catalytic [RuCl<sub>2</sub>(*p*-cymene)]<sub>2</sub>.<sup>9</sup> The intermediate ethoxyvinyl esters participate in intermolecular couplings with amines and alcohols to form amides and esters, respectively, under mildly acidic conditions. Application of these conditions to **31** provided a 40% yield of macrolactone **16** as shown in Scheme 4. More significantly, **16** was contaminated with only trace amounts of byproducts resulting from diene isomerization.

**Macrocyclization at C15–C16.** To complete the synthesis of the proposed structure of amphidinolide A from **16**, instal-

**Scheme 4.** Macrolactonization of **31**

lation of the C21–C25 epoxide side chain remained. Although this appeared possible starting from **16**, a more convergent route was desired whereby incorporation of this side chain would be performed prior to macrocyclization. Keeping this in mind, we

(8) Kita, Y.; Maeda, H.; Omori, K.; Okuno, T.; Tamura, Y. *Synlett* **1993**, 273.(9) Trost, B. M.; Chisholm, J. D. *Org. Lett.* **2002**, *4*, 3743.

Scheme 5. Completion of the Synthesis of **1**

also realized that one of our original endgame strategies (shown in Figure 1) utilizing a macrocyclization of **3** at C15–C16 had been unexplored up to this point and appeared tantalizing. One initial concern with this approach was the envisioned coupling of alkyne **6** with alkene **5** due to the possibility of undesirable self-condensation of **6**, which also contained a reactive terminal alkene. To address this concern, it was anticipated that an excess of the C1–C6 partner **24** would be required. The alkene partner ethyl ester **24** was replaced with Fmoc ester **5**, which was anticipated to cleave to the corresponding acid under more mild conditions, thereby avoiding a potentially low yielding hydrolysis step similar to the hydrolysis of **30**.<sup>10</sup> Application of the conditions used for the conversion of **29** to **30**—with an increase in the equivalents of alkene partner **5**—gave **32** along with its linear isomer as a minor product in 46% yield (76% brsm, Scheme 5). Deprotection of the Fmoc ester with piperidine in  $\text{CH}_2\text{Cl}_2$  provided acid **33** in 90% yield with no detectable alkene isomerization by  $^1\text{H}$  NMR. Esterification of **33** with **7** under the Kita conditions gave ester **3** in 66% yield. Despite the failure of **15** to undergo macrocyclization, the reaction of **3** proceeded smoothly with 10 mol %  $[\text{CpRu}(\text{MeCN})_3]\text{PF}_6$  in DCE, to provide macrolide **34** in 58% yield. Given the high degree of unsaturation present in this substrate, the chemoselectivity of this process is remarkable. The reason for the stark difference in reactivity between **3** and **15** is not clear; however, differences in conformational mobility may be a factor. Deprotection of **34** under acidic conditions provided **1**, which was identical by  $^1\text{H}$  NMR to the material prepared by Maleczka<sup>11</sup> and Pattenden,<sup>12</sup> and as anticipated did not match the spectroscopic data

reported by Kobayashi.<sup>13,14</sup> As shown in Table 2, there are significant deviations in the  $^1\text{H}$  NMR between **1** and the natural material.

At this juncture, we were intrigued with the opportunity to elucidate the correct structure of amphidinolide A. There are numerous examples in the literature where the total synthesis of a complex natural product reveals the structure was determined incorrectly.<sup>15</sup> Unfortunately, only an extremely small sample of natural amphidinolide A remains;<sup>16</sup> thus, additional NMR experiments are not possible. Therefore, total synthesis represents the only practical method by which the correct structure can be determined unambiguously.

Since the relative stereochemistry of **1** was assigned with NOE data measured on a macrolide possessing considerable flexibility, an error in the relative stereochemistry and not gross structure seemed most likely. This conclusion is also supported by a comparison of the spectral data for the natural material and the synthetic compound **1**. The differences in chemical shifts and coupling constants are not as large as would be expected for an error in connectivity.

Initially, it was assumed that the error in relative stereochemistry was in the epoxide region, as opposed to the tetrol, where the acyclic nature of the side chain would result in the least reliable NOE data. The *trans* stereochemistry of the epoxide was assumed to be correct on the basis of a good correlation between the reported  $J_{\text{H}20/\text{H}21}$  value and other *trans*-epoxides. An error in the relative stereochemistry of the epoxide was

(10) (a) Kessler, H.; Siegmeyer, R. *Tetrahedron Lett.* **1983**, *24*, 281. (b) Bednarek, M. A.; Bodansky, M. *Int. J. Pept. Protein Res.* **1983**, *21*, 196.

(11) Maleczka, R. E.; Terrell, L. R.; Geng, F.; Ward, J. S. *Org. Lett.* **2002**, *4*, 2841.

(12) Lam, H. W.; Pattenden, G. *Angew. Chem., Int. Ed.* **2002**, *41*, 508.

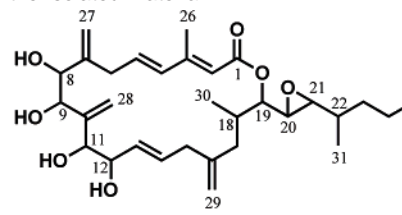
(13) (a) Kobayashi, J.; Ishibashi, M.; Nakamura, H.; Ohizumi, Y.; Yamasu, T.; Sasaki, T.; Hirata, Y. *Tetrahedron Lett.* **1986**, *27*, 5755. (b) Kobayashi, J.; Ishibashi, M.; Hirota, H. *J. Nat. Prod.* **1991**, *54*, 1435.

(14) Trost, B. M.; Chisholm, J. D.; Wroblewski, S. T.; Jung, M. *J. Am. Chem. Soc.* **2002**, *124*, 12420.

(15) For a comprehensive review, see: Nicolaou, K. C.; Snyder, S. A. *Angew. Chem., Int. Ed.* **2005**, *44*, 1012.

(16) Professor J. Kobayashi, personal communication.

**Table 2.** Deviation of the  $^1\text{H}$  NMR Chemical Shifts of Isomers **1**, **36**, **38**–**41**, **54**, **56**, **57**, and **59** Relative to the Values Reported for the Isolated Material<sup>a</sup>



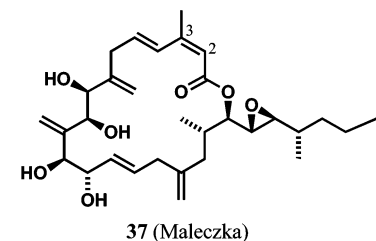
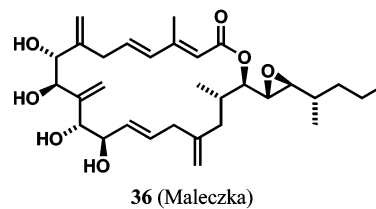
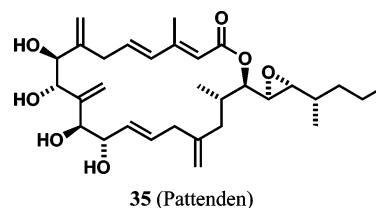
Proton	$\delta$ Synthetic Isomer – $\delta$ Isolated Material									
	1	36	38	39	40	54	41	56	57	59
2	0.00	0.00	-0.01	+0.02	+0.02	-0.03	-0.08	-0.01	+0.05	0.00
4	-0.07	-0.13	-0.08	-0.08	-0.11	-0.11	-0.11	-0.07	-0.01	+0.01
5	0.00	-0.03	-0.01	-0.01	-0.01	-0.01	-0.06	-0.01	-0.01	+0.01
6	+0.02	-0.01	+0.02	+0.05	+0.01	+0.01	-0.04	+0.02	0.00	+0.01
6'	-0.01	-0.17	-0.02	-0.13	-0.15	-0.15	-0.09	-0.19	-0.03	-0.02
8	-0.19	-0.05	-0.19	-0.10	-0.04	-0.04	-0.06	0.00	-0.01	+0.01
9	-0.29	-0.49	-0.30	-0.42	-0.48	-0.46	-0.28	-0.30	+0.04	+0.01
11	-0.25	-0.21	-0.26	-0.14	-0.20	-0.18	-0.10	-0.07	-0.05	-0.03
12	-0.01	-0.06	-0.02	-0.13	-0.05	-0.04	+0.05	-0.05	-0.02	0.00
13	-0.23	-0.15	-0.25	-0.03	-0.13	-0.10	+0.02	-0.09	-0.02	-0.01
14	+0.07	-0.02	+0.06	+0.03	-0.01	0.00	+0.06	-0.01	-0.01	0.00
15	+0.01	-0.05	0.00	-0.01	-0.03	-0.02	+0.05	-0.02	-0.03	0.00
15'	-0.10	-0.15	0.00	-0.01	-0.13	-0.10	-0.08	-0.09	-0.03	0.00
17	+0.18	+0.06	+0.16	-0.18	+0.05	-0.09	-0.20	+0.15	+0.16	-0.01
17'	-0.14	-	-0.13	-0.27	-0.10	-0.04	-0.16	-0.11	-0.07	0.00
18	-0.02	-	-0.04	-0.23	-0.06	-0.03	-0.16	-0.07	-0.05	-0.01
19	-0.17	-0.14	-0.11	-0.12	-0.05	-0.05	-0.16	-0.10	-0.07	0.00
20	+0.07	+0.05	+0.12	+0.17	+0.12	-0.01	+0.06	+0.07	+0.07	0.00
21	-0.06	-0.10	-0.07	-0.04	-0.10	+0.01	-0.06	-0.08	-0.08	0.00
26	+0.03	-0.04	+0.02	-0.01	-0.02	-0.03	-0.03	-0.01	0.00	0.00
27	+0.09	-0.06	+0.01	-0.02	-0.04	-0.03	-0.03	+0.01	-0.02	0.00
27'	+0.02	-0.03	+0.01	+0.03	-0.01	0.00	-0.01	+0.03	-0.02	0.00
28	+0.10	-0.03	+0.10	0.00	-0.02	-0.01	0.00	+0.02	-0.04	0.00
28'	+0.21	0.00	+0.20	+0.07	+0.02	+0.02	+0.05	+0.06	-0.03	+0.01
29	-0.01	-0.05	-0.02	-0.05	+0.03	-0.01	-0.14	-0.04	-0.03	0.00
29'	-0.01	-0.04	-0.01	-0.04	-0.02	0.00	-0.06	-0.03	-0.02	0.00
30	-0.07	-	-0.07	-0.02	-0.05	-0.01	-0.04	-0.08	-0.06	0.00
31	+0.05	-	+0.08	+0.07	+0.07	-0.04	0.00	+0.04	+0.04	0.00

<sup>a</sup> Spectra were measured in  $\text{CDCl}_3$  at 500 MHz. Differences are reported in parts per million. Values in black represent deviations of  $<0.04$ , blue 0.04–0.10, green 0.11–0.20, and red  $>0.20$

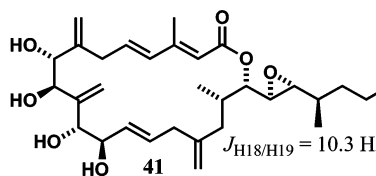
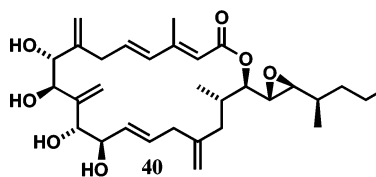
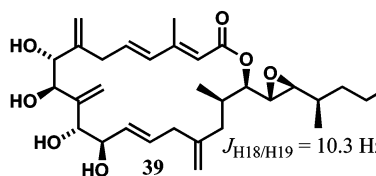
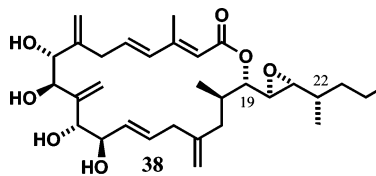
addressed by Pattenden, who reported the synthesis of epoxide epimer **35**, but it failed to match the spectroscopic data of the natural product.<sup>12</sup>

An error in correlating the tetrol and epoxide portions, which was determined stepwise by NOE from H11 to H13, from H13 to H15, and finally from H15 to H18, was considered by Maleczka.<sup>11</sup> However, as shown in Table 2, isomer **36** did not match the natural product. Finally, the possibility of the trisubstituted (*E*)-alkene being the source of the error was ruled out by Maleczka, who prepared (*Z*)-alkene **37**.<sup>11</sup>

**Synthesis of Isomers Derived from 6.** Although the most obvious structures had been ruled out by Pattenden and Maleczka, our attention remained focused on the epoxide portion.<sup>17</sup> The most logical targets were C22 epimer **38** and the isomer **39** from inversion of the C19–C21 triad. Using the endgame established for the synthesis of **1**, **38** and **39** were prepared. Although neither matched the data reported for the

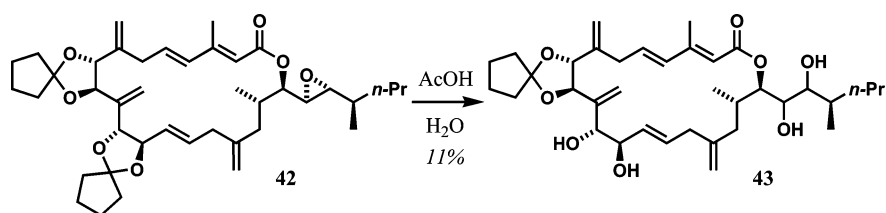
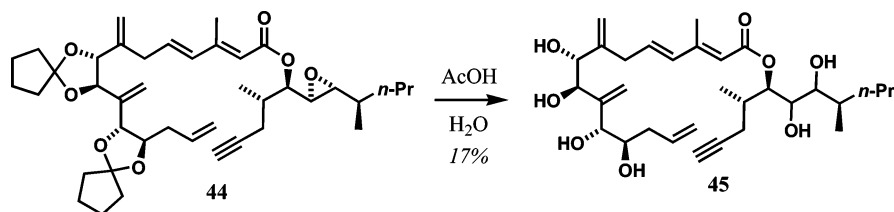
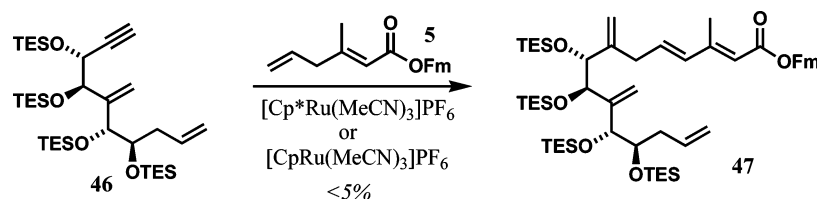


natural product (Table 2), the  $J_{\text{H18/H19}}$  value for **39** was 10.3 Hz, whereas the values for **1**, **36**, **38**, and the natural product were 3.3–3.8 Hz, thus suggesting the requirement for *trans* (as drawn) C18–C19 stereochemistry.



Proceeding on the belief that the correlation of the tetrol to the epoxide was tenuous at best, isomers **40**, **41**, and **54** were targeted, combining changes in the epoxide with a change in tetrol configuration. Although **40** and **41** were prepared uneventfully using the endgame established for **1**, the hydrolysis of **42** proved to be very problematic. As shown in Scheme 6,

(17) Trost, B. M.; Harrington, P. E. *J. Am. Chem. Soc.* **2004**, *126*, 5028.

Scheme 6. Attempted Conversion of **42** to **54**Scheme 7. Hydrolysis of **44**Scheme 8. Alkene–Alkyne Coupling of **46** with **5**

exposure of **42** to aqueous acetic acid failed to provide **54**. A number of byproducts were produced including tetrol **43**, which was isolated in 11% yield as a single diastereomer.<sup>18,19</sup> Other byproducts were isolated that appeared to be derived from hydrolysis of the epoxide in **42** before complete cleavage of the ketals. A wide variety of conditions were screened for the conversion of **42** to **54**; however, all resulted in hydrolysis of the epoxide before complete deprotection of the tetrol.

It was suspected that the ketals in *seco*-alkyne **44** might be more easily hydrolyzed than was the case for **42**. In the event, exposure of **44** to aqueous acetic acid gave hexol **45** as the major product in 17% yield as a single diastereomer (Scheme 7).<sup>19</sup> Products analogous to **43** were also isolated from the reaction.

In light of the difficulty encountered for the conversion of **42** to **54**, a new route to **54** was pursued. The TES group was chosen to replace the problematic cyclopentylidene ketals. Silyl ether **46** was prepared from **6** by hydrolysis with aqueous acetic acid followed by silylation with (TES)OTf. Somewhat surprisingly, alkene–alkyne coupling of **46** with **5** catalyzed by either [CpRu(MeCN)<sub>3</sub>]PF<sub>6</sub> or [Cp\*Ru(MeCN)<sub>3</sub>]PF<sub>6</sub> gave only trace amounts of **47** (Scheme 8). Alternatively, acid **49** was prepared in good yield as shown in Scheme 9. Hydrolysis of **33** followed by TES protection gave silyl ether **49** in 75% yield from **33**. Ester formation was lower yielding than was the case for ketal-protected acid **33**. The formation of ester **51** was accompanied by a number of byproducts as judged by <sup>1</sup>H NMR and TLC analysis of the crude reaction mixture. However, alkene–alkyne coupling of **51** catalyzed by either [CpRu(MeCN)<sub>3</sub>]PF<sub>6</sub> or [Cp\*Ru(MeCN)<sub>3</sub>]PF<sub>6</sub> rapidly cleaved the TES groups in **51**. No products that appeared to be derived from macrocycle **52** were detected by <sup>1</sup>H NMR, and only partially desilylated byproducts were isolated.

As shown in Scheme 10, switching the order of the final two steps gave a modest yield of **54**; however, it should be noted that this substrate is quite challenging given all the unprotected and potentially reactive functionality present—four additional double bonds, four free OH groups, and a sensitive epoxide and ester. Although **54** did not match, it did provide a very good fit in the epoxide region, thus suggesting that the relative stereochemistry of the C18–C22 portion may be correct.

To this point, comparisons to the natural product were focused on coupling constants, and apart from the requirement for *trans* C18–C19 stereochemistry, little information was gleaned by this approach. As shown in Figure 2, there were no other obvious trends in the vicinal *J*<sub>H/H</sub> values that could be exploited to predict the relative stereochemistry in the epoxide region. Clearly, a new method for comparison was required.

Initially, little effort was expended in comparing differences in the proton chemical shifts of each isomer from those of the natural product. However, upon careful examination of the

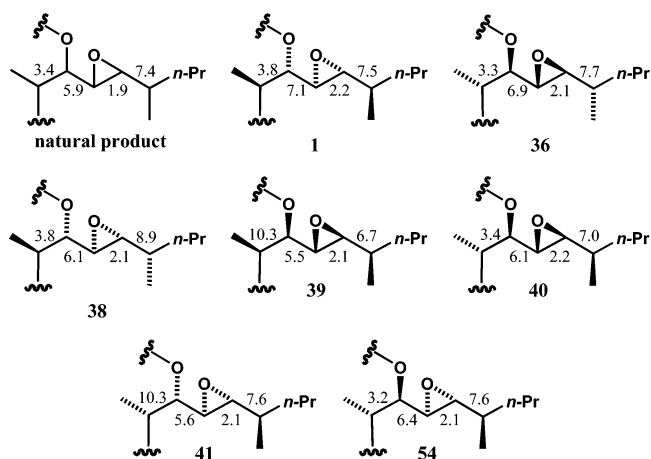
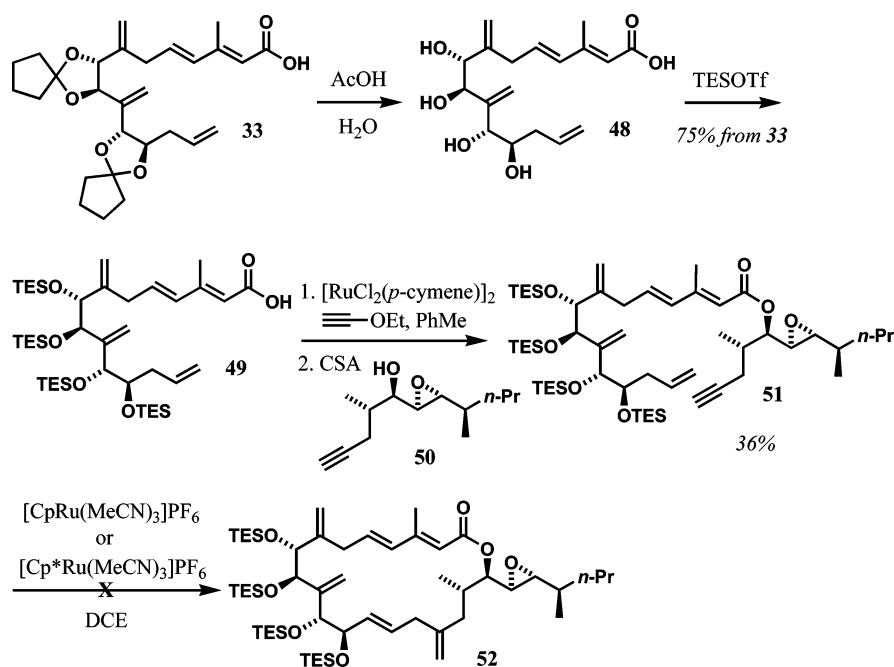
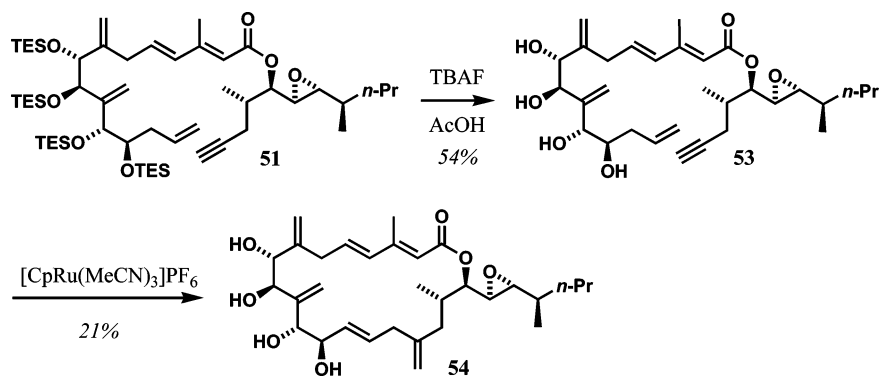


Figure 2. Comparison of the vicinal *J*<sub>H/H</sub> values (Hz).

(18) The location of the acetonide in **43** was not determined and is depicted arbitrarily for **43**.

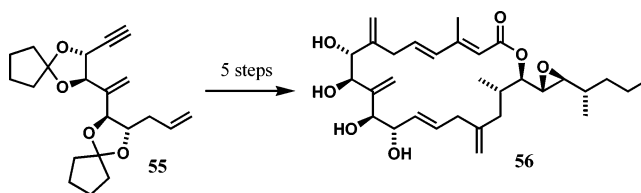
(19) The relative stereochemistry was not determined.



Scheme 9. Conversion of **33** to **51**Scheme 10. Macrocyclization of **53**

chemical shifts of various protons, a rather significant departure in the values relative to those of the natural product was observed. As shown in Table 2, this departure was most dramatic for the H<sub>9</sub> and H<sub>11</sub> protons. In addition, these differences were not random in sign or magnitude, but were consistently upfield relative to the values of the natural product. This was surprising since the variations were made in the epoxide region, where only small differences in the chemical shifts were observed in comparison to the large deviations in the tetrol region. In light of this realization, an error in the relative stereochemistry of the tetrol appeared likely.

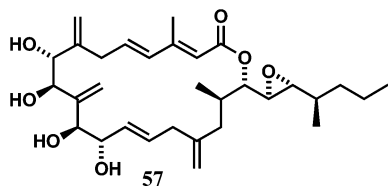
Although we were concerned that errors within the epoxide combined with the tetrol would make the possibilities so numerous that we would be faced with nearly an impossible task, key spectral data provided direction. Because the  $J_{H8/H9}$  and  $J_{H11/H12}$  values for **1**, **36**, **38–41**, and **54** were consistent with the natural product, it appeared likely that the relative stereochemistry of the diols was correct, but the stereochemistry of the C8–C9 diol was incorrect relative to that of the C11–C12 diol. Since H<sub>11</sub> was correlated stepwise to H<sub>18</sub> by NOE, whereas the C8–C9 diol was not correlated to the epoxide portion, the stereochemistry of the C11–C12 diol relative to

Scheme 11. Route to **56** via Alkene–Alkyne Coupling of **55** with **5**

the epoxide was assumed to be correct. Therefore, **56**, with the C8–C9 diol inverted, became the primary target.

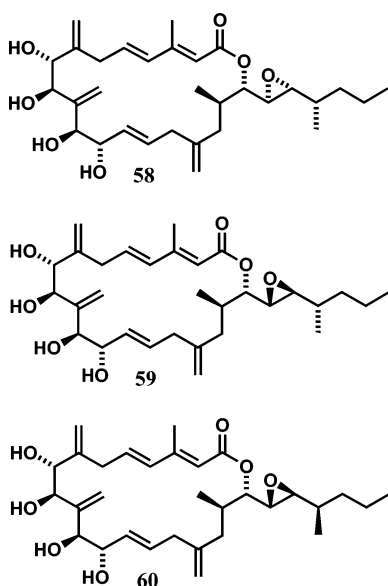
**Synthesis of Isomers Derived from 55.** Applying the same sequence that was used for the synthesis of **1** and **38–41**, isomer **56** was prepared uneventfully from **55** (Scheme 11). However, isomer **56**, with the C8–C9 diol inverted and epoxide stereochemistry of **1**, failed to match. Although the chemical shift of H<sub>11</sub> was closer than was the case for all the previous isomers, H<sub>9</sub> remained 0.30 ppm upfield from the natural product.

With these data, the combination of an error in the relative stereochemistry of the tetrol and epoxide appeared likely. Therefore, right-hand-side enantiomer **57** was targeted. Again, an identical sequence was used for the conversion of **55** to **57**. Although **57** did not match the natural product, the chemical



shifts in the tetrol region were extremely close to those of the natural product as shown in Table 2. Only in the epoxide region of **57** were the chemical shifts significantly different from those of the natural product.

Since the chemical shifts deviated significantly from those of the natural material only in the epoxide region, we assumed that the relative stereochemistry of the 20-membered ring of **57** matched that of the natural product. We continued to assume a *trans*-epoxide and *trans* H18/H19 stereochemistry. Therefore, only diastereomers **58**–**60** remained as possibilities. Isomer **58**,



the C22 epimer of **57**, did not seem a likely candidate given the differences in chemical shift that exist between **1** and **38**. Therefore, only **59** and **60** remained; however, **59** was the primary target given the analysis that follows. Isomer **54** provided the best overall fit in terms of chemical shift in the epoxide region of any isomer. This is the same relative stereochemistry in the epoxide region as found in **59**. The more quantitative analysis of the data in Table 2 that follows also pointed to **59**. The relationship between **57** and **59** is analogous to that between **36** and **54**, inversion of the C20–C22 triad. If the changes in chemical shift that occur when the C20–C22 triad of **36** is inverted, thus yielding **54**, are applied to **57**, a nearly perfect match to the natural material is obtained. For example, the chemical shift of H19 in **36** and **54** is 4.58 and 4.67 ppm, respectively. This represents a downfield shift of 0.09 ppm. The shift of H19 in **57** is 4.65 ppm. A 0.09 ppm downfield shift yields a predicted shift of 4.74 ppm for H19 of **59**. This value compares well with the shift of 4.72 ppm for H19 of the natural product. Analysis of the other protons yields similar results.

The first route to **59** is shown in Scheme 12. Ketal **61** was prepared from **55** via the standard route. As was the case for **42**, exposure of **61** to aqueous acid resulted in hydrolysis of

the epoxide in **61** before complete cleavage of the ketals. A variety of conditions were examined for the cleavage of the ketals; however, all failed to provide **59**. If the hydrolysis reactions were halted prior to the complete consumption of **61**, products analogous to **43** were detected in the crude reaction mixture by  $^1\text{H}$  NMR.

The second route to **59** that was pursued utilized an approach analogous to the one shown in Schemes 9 and 10 that was used to prepare **54**. Ketal **62** was hydrolyzed and converted to silyl ether **64** in 83% yield over two steps from **62** (Scheme 13). Ester formation gave **66** in 51% yield, and silyl cleavage with buffered TBAF provided **67** in 79% yield. However, treatment of **67** with catalytic  $[\text{CpRu}(\text{MeCN})_3]\text{PF}_6$  in DCE—the same conditions that were used to convert **53** to **54**—gave a multitude of byproducts. No products that appeared to be derived from **59** were detected in the crude reaction mixture by  $^1\text{H}$  NMR.

With the failure of **67** to provide even trace amounts of **59**, a model system for the conversion of **67** to **59** was examined. Alkyne **68** was chosen as a suitable model for **67**. As shown in Table 3, exposure of **68** to 10 mol %  $[\text{CpRu}(\text{MeCN})_3]\text{PF}_6$  in DCE gave a number of byproducts, but no **69** was isolated (Table 3, entry 1). Increasing the  $[\text{CpRu}(\text{MeCN})_3]\text{PF}_6$  loading to 1 equiv gave the desired macrocycle **69** in 8% yield (entry 2). Reaction of **68** in acetone gave a mixture of two products that appeared to be the two monoacetonides of **68**. Switching to the  $[\text{CpRu}(\text{COD})]\text{Cl}$  catalyst (entries 9–14) provided only trace amounts of **69** in MeOH and none in a mixed solvent of DMF/H<sub>2</sub>O (3:1).<sup>20</sup> Additives such as  $\text{NH}_4\text{PF}_6$  (entry 10) were not beneficial. Examination of the  $[\text{Cp}^*\text{Ru}(\text{MeCN})_3]\text{PF}_6$  catalyst proved to be worthwhile. Macrocycle **69** was isolated in modest yield from reactions conducted in DCE (entries 15 and 18) with  $[\text{Cp}^*\text{Ru}(\text{MeCN})_3]\text{PF}_6$ . Chloride ion was examined as an additive for coordination to the active catalyst, but no product was detected in the reaction (entry 19).

Application of the conditions shown in entry 18 to **67** provided **59** (Scheme 14). Given the extraordinary chemoselectivity required in this fully unprotected highly functionalized substrate, the modest yield is still gratifying. The spectral data for **59** provided an excellent fit to the natural product as shown in Table 2. One proton deviated by 0.03 ppm, one by 0.02 ppm, and the remainder by 0.01 ppm or less. The  $^1\text{H}$  NMR spectra in  $\text{C}_6\text{D}_6$  and  $\text{CD}_3\text{OD}$  deviated by 0.01 ppm or less from those of the natural product in those solvents. The  $J$  values in all three solvents were also in agreement. The  $^{13}\text{C}$  NMR spectrum deviated by 0.1 ppm or less in  $\text{CDCl}_3$ . These results are well within experimental error.<sup>21</sup> The optical rotation of  $[\alpha]^{24}_{\text{D}} +56$  ( $c$  0.05,  $\text{CHCl}_3$ ) was identical in sign to but slightly higher than the reported value of  $[\alpha]^{24}_{\text{D}} +46$  ( $c$  1.0,  $\text{CHCl}_3$ ), therefore establishing the absolute stereochemistry as shown for **59**. Finally, subsequent comparison of **59** and a sample of natural amphidinolide A by HPLC and NMR further confirmed the structural assignment.

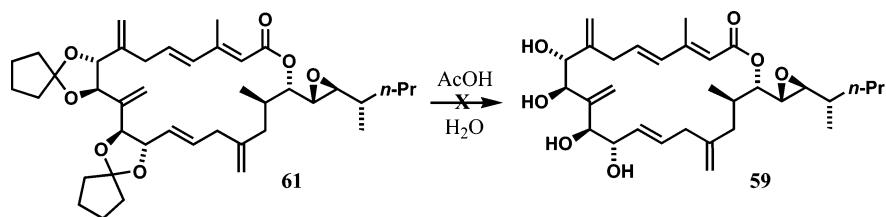
## Conclusion

We have used a combination of synthesis and NMR spectroscopy to determine the correct relative and absolute stereochemistries of amphidinolide A. Overall, 23 linear steps and

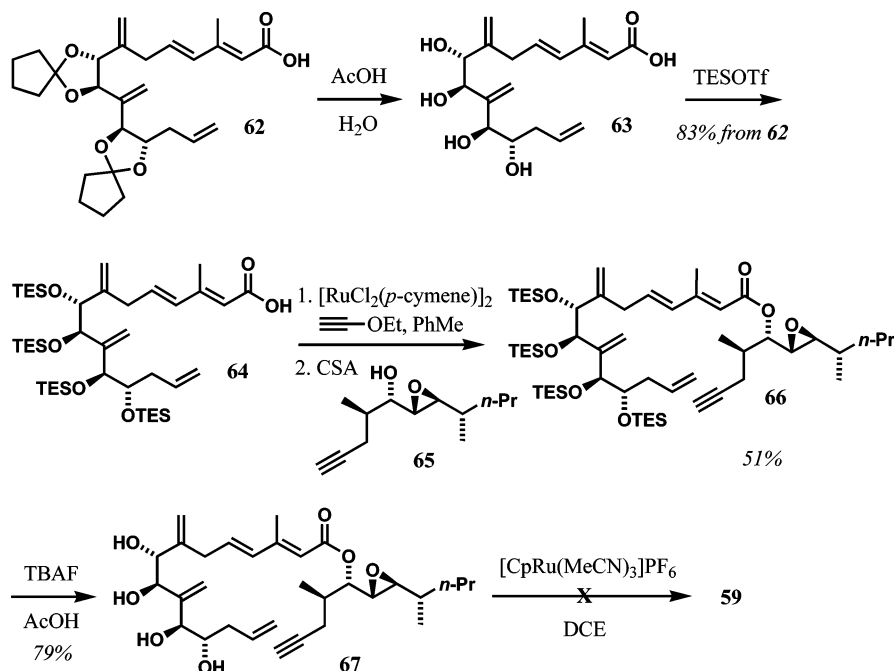
(20) Trost, B. M.; Probst, G. D.; Schoop, A. *J. Am. Chem. Soc.* **1998**, *120*, 9228.

(21) See the Supporting Information for a complete comparison of the spectroscopic data.

Scheme 12. Attempted Conversion of 61 to 59



Scheme 13. Second Route to 59



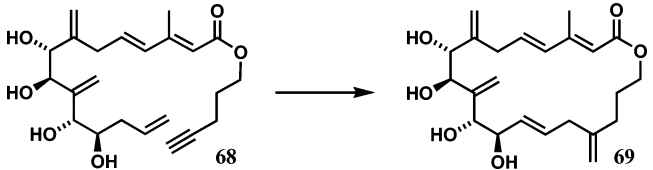
43 total steps were required to convert (–)-diethyl tartrate to amphidinolide A in an overall yield of 0.2%. A reliance on catalytic asymmetric processes allowed the building blocks for each isomer to be assembled with relative ease. Moreover, the convergent nature of the synthesis allowed these blocks to be assembled without an inordinate investment of time given the complexity of the targets. Finally, the remarkable ability of  $[\text{Cp}^*\text{Ru}(\text{MeCN})_3]\text{PF}_6$  to catalyze the macrocyclization of tetrol **67** clearly points to the potential power of the Ru-catalyzed alkene–alkyne coupling and warrants further study to determine the scope and generality of this transformation.

## Experimental Section

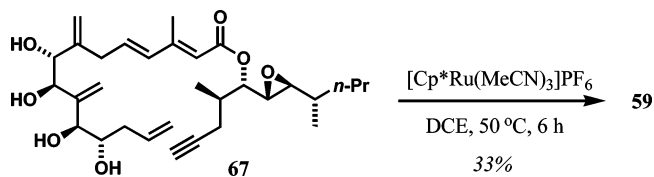
**9H-Fluoren-9-ylmethyl (2E,4E)-7-((2R,3R)-3-{1-[(2R,3R)-3-Allyl-1,4-dioxaspiro[4.4]non-2-yl]vinyl}-1,4-dioxaspiro[4.4]non-2-yl)-3-methylocta-2,4,7-trienoate (32).** Alkyne **6** (36 mg, 0.104 mmol) and alkene **5** (159 mg, 0.523 mmol) were dissolved in 300  $\mu\text{L}$  of dichloroethane and warmed to 50  $^\circ\text{C}$  in an oil bath, and  $[\text{Cp}^*\text{Ru}(\text{MeCN})_3]\text{PF}_6$  (5.1 mg, 0.01 mmol) was then added in one portion. After approximately 2 h, the reaction was placed atop a silica gel column. Purification by flash column chromatography on silica gel (10–30%  $\text{Et}_2\text{O}$  in petroleum ether) gave alkene **32** (31 mg, 46%) as a 3.5:1 mixture of branched and linear products. Further elution with 40–80%  $\text{CH}_2\text{Cl}_2$  in petroleum ether provided recovered alkyne **6** (11 mg, 30%) and alkene **5** (108 mg, 69%). Data for **32**:  $R_f = 0.41$  (20%  $\text{Et}_2\text{O}$  in petroleum ether); IR (film) 2958, 2877, 1714  $\text{cm}^{-1}$ ;  $^1\text{H}$  NMR (500 MHz,  $\text{CDCl}_3$ )  $\delta$  7.77 (d,  $J = 7.6$  Hz, 2H), 7.62 (d,  $J = 7.5$  Hz, 2H), 7.42 (t,  $J = 7.5$  Hz, 2H), 7.33 (t,  $J = 7.5$  Hz, 2H), 6.13–6.19 (m, 2H), 5.82–5.90 (m, 2H), 5.48 (s, 1H), 5.47 (s, 1H), 5.24 (s, 1H), 5.09–5.19 (m,

2H), 5.01 (s, 1H), 4.35–4.43 (m, 3H), 4.26 (t,  $J = 7.3$  Hz, 1H), 4.19 (d,  $J = 8.4$  Hz, 1H), 4.07 (d,  $J = 8.0$  Hz, 1H), 3.92 (m, 1H), 3.06 (dd,  $J = 15.4, 5.2$  Hz, 1H), 2.28 (s, 3H), 1.92–1.60 (m, 16H);  $^{13}\text{C}$  NMR (125 MHz,  $\text{CDCl}_3$ )  $\delta$  166.9, 152.8, 144.0, 143.3, 142.3, 141.2, 135.6, 134.2, 133.9, 127.7, 127.0, 125.1, 120.0, 119.0, 118.7, 118.0, 117.8, 117.4, 115.6, 84.0, 81.2, 79.7, 79.6, 65.8, 46.8, 37.6, 37.4, 37.3, 37.2, 36.3, 34.6, 23.5, 23.4, 23.3, 13.9; HRMS  $m/z$  calcd for  $\text{C}_{32}\text{H}_{32}\text{O}_4$  ( $\text{M}^+ - \text{C}_{10}\text{H}_{16}\text{O}_2$ ) 480.2301, found 480.2327.

**(2E,4E)-7-((2R,3R)-3-{1-[(2R,3R)-3-Allyl-1,4-dioxaspiro[4.4]non-2-yl]vinyl}-1,4-dioxaspiro[4.4]non-2-yl)-3-methylocta-2,4,7-trienoic Acid (33).** To a solution of ester **32** (401 mg, 0.62 mmol) in  $\text{CH}_2\text{Cl}_2$  (18 mL) at room temperature was added piperidine (2.1 mL, 1.8 g, 21 mmol). After 2.5 h at room temperature, the reaction mixture was diluted with ether, water, and 1 M HCl. The aqueous phase was extracted with ether (3 $\times$ ), and the combined organic extracts were washed with brine (1 $\times$ ), dried over  $\text{MgSO}_4$ , and concentrated. Purification by flash column chromatography on silica gel (40%  $\text{EtOAc}$  in petroleum ether) gave acid **33** (262 mg, 90%) as a colorless oil:  $R_f = 0.69$  (10%  $\text{MeOH}$  in  $\text{CHCl}_3$ ); IR (film) 3076, 2959, 1687  $\text{cm}^{-1}$ ;  $^1\text{H}$  NMR (500 MHz,  $\text{CDCl}_3$ )  $\delta$  6.15–6.22 (m, 2H), 5.80–5.88 (m, 1H), 5.75 (s br, 1H), 5.47 (s, 1H), 5.46 (s, 1H), 5.22 (s, 1H), 5.08–5.13 (m, 2H), 4.99 (s, 1H), 4.39 (d,  $J = 8.4$  Hz, 1H), 4.18 (d,  $J = 8.5$  Hz, 1H), 4.04 (d,  $J = 8.1$  Hz, 1H), 3.90 (dt,  $J = 7.9, 4.0$ , 1H), 3.05 (dd,  $J = 16.6, 4.4$  Hz, 1H), 2.89 (dd,  $J = 16.5, 5.0$  Hz, 1H), 2.39–2.44 (m, 1H), 2.29 (s, 3H), 2.24–2.29 (m, 1H), 1.62–1.93 (m, 17H);  $^{13}\text{C}$  NMR (125 MHz,  $\text{CDCl}_3$ )  $\delta$  172.2, 154.5, 143.2, 135.6, 134.8, 133.9, 119.1, 118.7, 117.8, 117.7, 117.4, 115.7, 84.0, 81.2, 79.7, 79.6, 37.6, 37.4, 37.3, 37.2, 36.3, 34.6, 23.5, 23.4, 23.2, 14.1; HRMS  $m/z$  calcd for  $\text{C}_{28}\text{H}_{38}\text{O}_6$  470.2668, found 470.2662; optical rotation  $[\alpha]^{23}_{\text{D}} +40.1$  (c 1.2,  $\text{CH}_2\text{Cl}_2$ ).

Table 3. Optimization of the Macrocyclization of **68**


entry	catalyst	concn (mol %)	solvent	concn (M)	additive	temp (°C)	yield (%)
1	[CpRu(MeCN) <sub>3</sub> ]PF <sub>6</sub>	11	DCE	0.001		50	0
2	[CpRu(MeCN) <sub>3</sub> ]PF <sub>6</sub>	109	DCE	0.001		50	8
3	[CpRu(MeCN) <sub>3</sub> ]PF <sub>6</sub>	10	acetone	0.001		50	0
4	[CpRu(MeCN) <sub>3</sub> ]PF <sub>6</sub>	12	DME	0.001		50	<5
5	[CpRu(MeCN) <sub>3</sub> ]PF <sub>6</sub>	16	THF	0.001		50	<5
6	[CpRu(MeCN) <sub>3</sub> ]PF <sub>6</sub>	100	THF	0.001		50	0
7	[CpRu(MeCN) <sub>3</sub> ]PF <sub>6</sub>	15	DMF	0.001		50	0
8	[CpRu(MeCN) <sub>3</sub> ]PF <sub>6</sub>	16	DCE/DMF (20:1)	0.001		50	<5
9	[CpRu(COD)]Cl	18	MeOH	0.001		60	<5
10	[CpRu(COD)]Cl	11	MeOH	0.05	NH <sub>4</sub> PF <sub>6</sub> (50 mol %)	60	<5
11	[CpRu(COD)]Cl	11	MeOH	0.01	AgPF <sub>6</sub> (50 mol %)	60	<5
12	[CpRu(COD)]Cl	9	MeOH	0.01	In(OTf) <sub>3</sub> (17 mol %)	60	<5
13	[CpRu(COD)]Cl	11	MeOH	0.01	LiCl (21 mol %)	60	<5
14	[CpRu(COD)]Cl	18	DMF/H <sub>2</sub> O (3:1)	0.001		80	0
15	[Cp*Ru(MeCN) <sub>3</sub> ]PF <sub>6</sub>	15	DCE	0.001		50	7
16	[Cp*Ru(MeCN) <sub>3</sub> ]PF <sub>6</sub>	15	DMF	0.001		50	0
17	[Cp*Ru(MeCN) <sub>3</sub> ]PF <sub>6</sub>	13	THF	0.001		50	<5
18	[Cp*Ru(MeCN) <sub>3</sub> ]PF <sub>6</sub>	25	DCE	0.001		50	31
19	[Cp*Ru(MeCN) <sub>3</sub> ]PF <sub>6</sub>	27	DCE	0.001	<i>n</i> -Bu <sub>4</sub> NCl (32 mol %)	50	0

Scheme 14. Macrocyclization of Tetrol **67**

(1*R*)-3-*O*-[(2*E*,4*E*)-7-((2*R*,3*R*)-3-[1-((2*R*,3*R*)-3-allyl-1,4-dioxaspiro[4.4]non-2-yl)vinyl]-1,4-dioxaspiro[4.4]non-2-yl)-3-methylocta-2,4,7-trienoyl]-1,2-anhydro-4,5-dideoxy-1-[(1*R*)-1-methylbutyl]-4-prop-2-yn-1-yl-*L*-arabinitol (**3**). Acid **33** (36 mg, 0.0764 mmol) and [RuCl<sub>2</sub>(*p*-cymene)]<sub>2</sub> (4.7 mg, 0.00764 mmol) were dissolved in 2 mL of toluene. Ethyl ethynyl ether (40% in hexanes, 20 μL, 0.084 mmol) was then added. After 2 h, the reaction was concentrated to a dark solid. Alcohol **7** (42 mg, 0.1997 mmol) was then added in 300 μL of dichloroethane, followed by a solution of CSA (1.8 mg, 0.00764 mmol) in 200 μL of dichloroethane. After 2 h, the reaction was quenched with 10 μL of Et<sub>3</sub>N and placed atop a silica gel column. Purification by silica gel chromatography (20–40% Et<sub>2</sub>O in petroleum ether) gave ester **3** (33 mg, 66%), recovered epoxide **7** (27 mg, 64%), and acid **33** (5.5 mg, 15%). Data for **3**: *R*<sub>f</sub> = 0.19 (10% Et<sub>2</sub>O in petroleum ether); IR (film) 3303, 2559, 2116 cm<sup>-1</sup>; <sup>1</sup>H NMR (500 MHz, CDCl<sub>3</sub>) δ 6.14 (s br, 2H), 5.81–5.89 (m, 1H), 5.75 (s, 1H), 5.47 (s, 1H), 5.46 (s, 1H), 5.22 (s, 1H), 2.08–5.13 (m, 2H), 4.98 (s, 1H), 4.83 (t, *J* = 6.0 Hz, 1H), 4.38 (t, *J* = 8.5 Hz, 1H), 4.18 (d, *J* = 8.5 Hz, 1H), 4.04 (d, *J* = 8.1 Hz, 1H), 3.88 (m, 1H), 3.03 (d, *J* = 16.5 Hz, 1H), 2.92 (dd, *J* = 6.0, 2.2 Hz, 1H), 2.88 (dd, *J* = 15.9, 4.4 Hz, 1H), 2.68 (dd, *J* = 7.4, 2.2 Hz, 1H), 2.36–2.44 (m, 2H), 2.35 (dd, *J* = 5.1 Hz, 1H), 2.29 (s, 3H), 2.22–2.28 (m, 2H), 2.05–2.11 (m, 1H), 2.05–2.11 (m, 1H), 2.01 (t, *J* = 2.7 Hz, 1H), 1.59–1.90 (m, 13H), 1.20–1.46 (m, 6H), 1.13 (d, *J* = 7.0 Hz, 3H), 0.93 (d, *J* = 6.8 Hz, 3H), 0.88 (t, *J* = 7.2 Hz, 3H); <sup>13</sup>C NMR (125 MHz, CDCl<sub>3</sub>) δ 166.1, 153.2, 143.3, 142.4, 135.6, 134.2, 133.9, 119.0, 118.7, 117.8, 117.4, 115.6, 84.1, 81.8, 81.2, 79.7, 79.6, 74.7, 70.2, 61.5, 56.8, 51.0, 37.6, 37.5, 37.4, 37.3, 37.2, 36.6, 36.2, 35.3, 35.1, 34.6, 29.7, 23.5, 23.4, 23.3, 20.0, 15.8, 15.2, 14.2; HRMS *m/z* calcd for C<sub>41</sub>H<sub>58</sub>O<sub>7</sub> 662.4183, found 662.4187; optical rotation [α]<sub>D</sub><sup>25</sup> +30.9 (*c* 0.75, CH<sub>2</sub>Cl<sub>2</sub>).

(3*a'R*,4*a'R*,7*a'R*,16'*S*,17'*R*,22*a'R*)-12',17'-Dimethyl-16'-{(2*S*,3*R*)-3-[(1*R*)-1-methylbutyl]oxiran-2-yl]-4',8',19'-tris(methylene)-3*a'*,4',-4*a'*,7*a'*,8',9',16',17',18',1 9',20',22*a'*-dodecahydro-14'*H*-dispiro[cyclopentane-1,2'-bis[1,3]dioxolo[4,5-*i*:4',5'-*I*]oxacycloicosine-6',1'-cyclopentane]-14'-one (**34**). Ester **34** (24 mg, 0.0362 mmol) was dissolved in 36 mL of dichloroethane and the resulting solution warmed to 50 °C in an oil bath. [CpRu(MeCN)<sub>3</sub>]PF<sub>6</sub> was then added. After 1 h, the reaction was quenched with the addition of 50 μL of Et<sub>3</sub>N and concentrated. Purification by flash column chromatography on silica gel (10–30% Et<sub>2</sub>O in petroleum ether) gave **34** (14 mg, 58%) as a yellow oil: *R*<sub>f</sub> = 0.32 (20% Et<sub>2</sub>O in petroleum ether); IR (film) 2958, 1714 cm<sup>-1</sup>; <sup>1</sup>H NMR (500 MHz, CDCl<sub>3</sub>) δ 6.16 (d, *J* = 16.0 Hz, 1H), 6.07–6.13 (m, 1H), 5.79 (s br, 1H), 5.75 (t, *J* = 7.4 Hz, 1H), 5.54 (s, 1H), 5.50 (s, 1H), 5.29 (s, 1H), 5.25 (dd, *J* = 15.1, 7.3 Hz, 1H), 5.17 (s, 1H), 4.80 (s, 1H), 4.71 (s, 1H), 5.54 (dd, *J* = 7.2, 3.7 Hz), 4.28 (d, *J* = 8.2 Hz, 1H), 4.20 (d, *J* = 8.3 Hz, 1H), 4.13 (t, *J* = 7.7 Hz, 1H), 3.85 (d, *J* = 7.8 Hz, 1H), 3.16 (dd, *J* = 13.8, 8.8 Hz, 1H), 3.03 (dd, *J* = 14.0, 5.0 Hz, 1H), 2.96 (dd, *J* = 7.2, 2.2 Hz, 1H), 2.71 (dd, *J* = 7.3, 2.1 Hz, 1H), 2.55–2.66 (m, 2H), 2.44 (dd, *J* = 13.8, 6.0 Hz, 1H), 2.30 (s, 3H), 2.12–2.18 (m, 1H), 1.80–1.95 (m, 8H), 1.62–1.79 (m, 8H), 1.22–1.56 (m, 6H), 1.04 (d, *J* = 7.2 Hz, 3H), 0.99 (d, *J* = 6.8 Hz, 3H), 0.93 (t, *J* = 7.2 Hz, 3H); <sup>13</sup>C NMR (125 MHz, CDCl<sub>3</sub>) δ 166.0, 151.9, 146.0, 143.1, 142.5, 135.3, 135.2, 133.9, 133.3, 127.9, 118.9, 118.8, 117.2, 115.1, 111.7, 84.9, 82.3, 81.1, 78.2, 77.7, 61.5, 54.4, 39.3, 38.1, 37.6, 37.4, 37.3, 37.1, 36.7, 35.7, 35.5, 33.9, 29.7, 23.5, 23.4, 23.3, 23.3, 19.9, 17.2, 16.0, 14.3; HRMS *m/z* calcd for C<sub>41</sub>H<sub>58</sub>O<sub>7</sub> 662.4183, found 662.4179; optical rotation [α]<sub>D</sub><sup>25</sup> +59.6 (*c* 1.0, CH<sub>2</sub>Cl<sub>2</sub>).

(+)-Amphidinolide **A** (Proposed Structure, **1**). Ketal **34** (7.6 mg, 0.0115 mmol) was suspended in 300 μL of dioxane, and 200 μL of water was added. Amberlyst-15 (15 mg, 0.0705 mmol) was then added, and the reaction was warmed to 60 °C. After 60 h, additional Amberlyst-15 (30 mg, 0.141 mmol) was added and the temperature raised to 85 °C. After 6 h, the reaction was filtered and concentrated. The residue was purified by HPLC (70% ethyl acetate in hexanes) to provide **1** (3.7 mg, 61%) as a white foam: *R*<sub>f</sub> = 0.41 (ethyl acetate); IR (film) 3384, 3284, 2922, 1714 cm<sup>-1</sup>; <sup>1</sup>H NMR (500 MHz, CDCl<sub>3</sub>) δ 6.18 (d, *J* = 15.6 Hz, 1H), 6.04–6.10 (m, 1H), 5.79 (s, 1H), 5.72–5.76 (m,

1H), 5.59 (s, 1H), 5.58 (s, 1H), 5.36 (s, 1H), 5.25 (d,  $J = 13.4$  Hz, 1H), 4.86 (s, 1H), 4.77 (s, 1H), 4.53 (dd,  $J = 7.2, 3.8$  Hz, 1H), 4.28 (s, 1H), 4.21 (d,  $J = 7.2$  Hz, 1H), 3.82 (s, 1H), 3.22 (bd,  $J = 14.9, 1H$ ), 3.11 (t,  $J = 15.5, 1H$ ), 2.91 (d,  $J = 6.2$  Hz, 1H), 2.74 (d br,  $J = 13.8$  Hz, 1H), 2.63–2.70 (m, 3H), 2.52 (d,  $J = 12.5$  Hz, 1H), 2.34 (s br, 1H), 2.29 (s, 3H), 2.11–2.20 (m, 2H), 2.01–2.09 (m, 1H), 1.77 (t,  $J = 11.8$  Hz, 1H), 1.10–1.60 (m, 6H), 0.97 (d,  $J = 6.7$  Hz, 3H), 0.86–0.92 (m, 6H);  $^{13}\text{C}$  NMR (125 MHz,  $\text{CDCl}_3$ )  $\delta$  165.6, 152.0, 145.2, 136.3, 134.9, 131.1, 130.2, 119.3, 115.4, 114.8, 113.8, 96.1, 94.3, 73.4, 72.5, 70.9, 69.6, 61.4, 60.4, 54.2, 38.5, 36.7, 35.4, 33.3, 31.9, 29.7, 29.3, 22.7, 22.3, 21.0, 14.2; optical rotation  $[\alpha]^{23}_{\text{D}} = +55.8$  (c 0.2,  $\text{CH}_2\text{Cl}_2$ ).

**(2E,4E,8R,9R,11S,12S)-3-Methyl-7,10-bis(methylene)-8,9,11,12-tetrakis(triethylsilyloxy)pentadeca-2,4,14-trienoic Acid (64).** To ketal **62** (76 mg, 0.16 mmol) at room temperature were added acetic acid (1.5 mL) and water (500  $\mu\text{L}$ ). The reaction mixture was heated to 40 °C for 20 h and concentrated to give tetrol **63**, which was used in the next step without further purification. To a solution of tetrol **63**, prepared in the previous step, in THF (4 mL) at 0 °C were added *i*-Pr<sub>2</sub>NEt (260  $\mu\text{L}$ , 193 mg, 1.5 mmol) and (TES)OTf (230  $\mu\text{L}$ , 269 mg, 1.0 mmol). The reaction mixture was stirred at 0 °C for 10 min, quenched with 1 M HCl, stirred for 10 min, and diluted with ether and water. The aqueous phase was extracted with ether (3 $\times$ ), and the combined organic extracts were washed with saturated  $\text{KH}_2\text{PO}_4$  (1 $\times$ ) and brine (1 $\times$ ), dried over  $\text{MgSO}_4$ , and concentrated. Purification by flash column chromatography on silica gel (5–10% EtOAc in petroleum ether) gave silyl ether **64** (106 mg, 83%) as a colorless oil:  $R_f = 0.56$  (30% EtOAc in petroleum ether); IR (film) 2956, 1684, 1610, 1096, 738  $\text{cm}^{-1}$ ;  $^1\text{H}$  NMR (500 MHz,  $\text{CDCl}_3$ )  $\delta$  6.20 (ddd,  $J = 15.6, 6.8, 6.8$  Hz, 1H), 6.14 (d,  $J = 15.6$  Hz, 1H), 5.82 (dddd,  $J = 17.0, 14.3, 10.3, 7.1$  Hz, 1H), 5.40–5.39 (m, 2H), 5.09 (s, 1H), 5.05 (dd,  $J = 9.6, 2.0$  Hz, 1H), 5.02 (d,  $J = 0.9$  Hz, 1H), 4.79 (d,  $J = 1.3$  Hz, 1H), 4.26 (d,  $J = 4.0$  Hz, 1H), 4.23 (d,  $J = 3.8$  Hz, 1H), 4.21 (d,  $J = 3.7$  Hz, 1H), 3.80 (ddd,  $J = 7.9, 3.9, 3.9$  Hz, 1H), 3.01 (dd,  $J = 17.5, 6.6$  Hz, 1H), 2.95 (dd,  $J = 17.2, 6.6$  Hz, 1H), 2.40 (dm,  $J = 14.2$  Hz, 1H), 2.31 (d,  $J = 1.1$  Hz, 3H), 2.30 (m, 1H), 2.14 (ddd,  $J = 15.4, 7.7, 7.7$  Hz, 1H), 0.99–0.91 (m, 36H), 0.65–0.51 (m, 24H), exchangeable proton not listed;  $^{13}\text{C}$  NMR (126 MHz,  $\text{CDCl}_3$ )  $\delta$  171.6, 155.0, 148.7, 146.5, 136.4, 136.1, 135.0, 117.2, 116.9, 116.6, 112.9, 78.1, 75.9, 75.8, 75.0, 37.1, 35.4, 14.0, 7.1, 7.05, 7.04, 7.01, 5.4, 5.32, 5.28, 5.1; optical rotation  $[\alpha]^{23}_{\text{D}} = -1.3$  (c 0.20,  $\text{CH}_2\text{Cl}_2$ ).

**(5S)-4,5-Anhydro-1,2-dideoxy-3-O-[(2E,4E,8R,9R,11S,12S)-3-methyl-7,10-bis(methylene)-8,9,11,12-tetrakis(triethylsilyloxy)pentadeca-2,4,14-trienoyl]-5-[(1S)-1-methylbutyl]-2-prop-2-yn-1-yl-D-ribitol (66).** To a solution of acid **64** (170 mg, 0.21 mmol) in PhMe (3.0 mL) at room temperature were added  $[\text{RuCl}_2(p\text{-cymene})_2]$  (12 mg, 0.020 mmol) and ethoxyacetylene (60  $\mu\text{L}$ , 50 wt % in hexanes, 0.34 mmol). The reaction mixture was stirred at room temperature for 2 h and concentrated under a stream of argon. A solution of alcohol **65** (108 mg, 0.51 mmol) in DCE (2.5 mL) was added via cannula followed by CSA (5.1 mg, 22  $\mu\text{mol}$ ). The reaction mixture was stirred at room temperature for 2 h, filtered through silica gel, and concentrated. Purification by flash column chromatography on silica gel (from 1% to 2% to 5% to 20% EtOAc in petroleum ether) gave ester **66** (108 mg, 51%) as a colorless oil:  $R_f = 0.36$  (5% EtOAc in petroleum ether); IR (film) 3312, 2946, 1714, 1605, 1146, 1094, 741  $\text{cm}^{-1}$ ;  $^1\text{H}$  NMR (500 MHz,  $\text{CDCl}_3$ )  $\delta$  6.20–6.10 (m, 2H), 5.82 (dddd,  $J = 17.2, 14.4, 10.3, 7.3$  Hz, 1H), 5.71 (s, 1H), 5.40–5.39 (m, 2H), 5.08 (s, 1H), 5.05 (dm,  $J = 9.0$  Hz, 1H), 5.02 (d,  $J = 1.2$  Hz, 1H), 4.79 (d,  $J = 1.5$  Hz, 1H), 4.70 (dd,  $J = 6.7, 4.3$  Hz, 1H), 4.26 (d,  $J = 4.0$  Hz, 1H), 4.23 (d,  $J = 3.7$  Hz, 1H), 4.21 (d,  $J = 3.5$  Hz, 1H), 3.80 (ddd,  $J = 8.2, 3.9, 3.9$  Hz, 1H), 3.00 (dd,  $J = 16.6, 5.7$  Hz, 1H), 2.94 (dd,  $J = 17.2, 6.4$  Hz, 1H), 2.82 (dd,  $J = 7.5, 2.2$  Hz, 1H), 2.75 (dd,  $J = 6.7, 2.1$  Hz, 1H), 2.40 (dm,  $J = 14.2$  Hz, 1H), 2.34 (ddd,  $J = 15.9, 5.5, 2.7$  Hz, 1H), 2.29 (d,  $J = 1.1$  Hz, 3H), 2.19 (dd,  $J = 7.9, 2.7$  Hz, 1H), 2.16–2.11 (m, 2H), 1.98 (t,  $J = 2.7$  Hz, 1H), 1.49–1.22 (m, 5H),

1.14 (d,  $J = 6.6$  Hz, 3H), 0.98–0.92 (m, 39H), 0.88 (t,  $J = 6.7$  Hz, 3H), 0.65–0.55 (m, 24H);  $^{13}\text{C}$  NMR (126 MHz,  $\text{CDCl}_3$ )  $\delta$  166.1, 153.5, 148.8, 146.5, 136.5, 135.5, 135.0, 117.2, 117.0, 116.6, 112.8, 82.3, 78.0, 75.9, 74.9, 74.2, 69.9, 69.6, 62.6, 55.7, 37.1, 36.6, 35.4, 35.2, 35.0, 22.4, 20.0, 15.7, 15.6, 14.3, 14.2, 7.12, 7.09, 7.06, 7.0, 5.4, 5.30, 5.27, 5.1; ESIMS  $m/z$  calcd for  $\text{C}_{55}\text{H}_{103}\text{O}_7\text{Si}_4$  ( $\text{M}^+ + \text{H}$ ) 987.7, found 987.1; optical rotation  $[\alpha]^{23}_{\text{D}} = -18$  (c 0.50,  $\text{CH}_2\text{Cl}_2$ ).

**(5S)-4,5-Anhydro-1,2-dideoxy-5-[(1R)-1-methylbutyl]-2-prop-2-yn-1-yl-3-O-[(2E,4E,8R,9R,11S,12S)-8,9,11,12-tetrahydroxy-3-methyl-7,10-bis(methylene)pentadeca-2,4,14-trienoyl]-D-ribitol (67).** To a solution of silyl ether **66** (45 mg, 0.046 mmol) in THF (1.0 mL) at room temperature was added 200  $\mu\text{L}$  of a mixture of TBAF (2.0 mL, 1 M in THF, 2.0 mmol) and acetic acid (115  $\mu\text{L}$ , 121 mg, 2.01 mmol). The reaction mixture was stirred at room temperature for 30 h and concentrated. Purification by flash column chromatography on silica gel (from 30% to 50% to 70% EtOAc in petroleum ether) gave tetrol **67** (19 mg, 79%) as a white foam:  $R_f = 0.54$  (EtOAc); IR (film from  $\text{CH}_2\text{Cl}_2$ ) 3424 (br), 3297, 2917, 1716, 1607, 1236, 1150  $\text{cm}^{-1}$ ;  $^1\text{H}$  NMR (500 MHz,  $\text{CDCl}_3$ )  $\delta$  6.19–6.14 (m, 2H), 5.85 (dddd,  $J = 16.8, 14.3, 10.6, 7.1$  Hz, 1H), 5.72 (d,  $J = 1.0$  Hz, 1H), 5.34 (s, 1H), 5.32 (s, 1H), 5.23 (s, 1H), 5.17 (dm,  $J = 7.2$  Hz, 1H), 5.14 (dd,  $J = 1.1, 1.1$  Hz, 1H), 5.02 (d,  $J = 1.0$  Hz, 1H), 4.71 (dd,  $J = 4.2, 2.1$  Hz, 1H), 4.33–4.31 (m, 2H), 4.17 (d,  $J = 4.9$  Hz, 1H), 3.83 (ddd,  $J = 8.3, 4.6, 4.6$  Hz, 1H), 3.03 (dd,  $J = 17.0, 4.9$  Hz, 1H), 2.92 (dd,  $J = 16.6, 4.4$  Hz, 1H), 2.80 (dd,  $J = 7.5, 2.1$  Hz, 1H), 2.75 (dd,  $J = 6.5, 2.2$  Hz, 1H), 2.39 (dm,  $J = 14.2$  Hz, 1H), 2.33 (ddd,  $J = 16.2, 5.6, 2.8$  Hz, 1H), 2.26 (d,  $J = 1.1$  Hz, 3H), 2.25 (dd,  $J = 14.5, 8.1$  Hz, 1H), 2.18 (dd,  $J = 4.3, 2.7$  Hz, 1H), 2.13 (m, 1H), 1.98 (t,  $J = 2.7$  Hz, 1H), 1.48–1.21 (m, 5H), 1.13 (d,  $J = 6.7$  Hz, 3H), 0.88 (t,  $J = 7.2$  Hz, 3H), 0.87 (d,  $J = 6.7$  Hz, 3H);  $^{13}\text{C}$  NMR (126 MHz,  $\text{CDCl}_3$ )  $\delta$  166.0, 152.9, 147.5, 146.3, 135.6, 134.24, 134.18, 118.5, 117.8, 116.7, 114.0, 82.2, 76.0, 74.8, 74.1, 73.0, 72.3, 69.8, 62.5, 55.6, 37.9, 36.6, 36.0, 35.2, 35.0, 22.5, 19.9, 15.6, 14.3, 14.2, 14.0; ESIMS  $m/z$  calcd for  $\text{C}_{31}\text{H}_{46}\text{O}_7\text{Na}$  ( $\text{M}^+ + \text{Na}$ ) 553.3, found 553.3; optical rotation  $[\alpha]^{29}_{\text{D}} = +4.8$  (c 0.10,  $\text{CH}_2\text{Cl}_2$ ).

**(+)-Amphidinolide A (Revised Structure, 59).** A solution of alkyne **67** (15.6 mg, 0.029 mmol) in DCE (30 mL) was degassed by bubbling nitrogen through the solution for 15 min. The reaction mixture was heated to 50 °C, and  $[\text{Cp}^*\text{Ru}(\text{MeCN})_3]\text{PF}_6$  (3.6 mg, 7.1  $\mu\text{mol}$ ) was added. After 6 h at 50 °C, the reaction mixture was filtered through silica gel and concentrated. Purification by flash column chromatography on silica gel (from 40% to 60% to 80% EtOAc in petroleum ether) gave (+)-amphidinolide A (**59**) (5.2 mg, 33%) and recovered alkyne **67** (1.9 mg, 12%) as amorphous solids. Data for (+)-amphidinolide A (**59**):  $R_f = 0.33$  (80% EtOAc in petroleum ether); IR (film from  $\text{CH}_2\text{Cl}_2$ ) 3438 (br), 2927, 1715, 1612, 1235, 1150, 850  $\text{cm}^{-1}$ ;  $^1\text{H}$  NMR (500 MHz,  $\text{CDCl}_3$ )  $\delta$  6.28 (d,  $J = 15.4$  Hz, 1H), 6.10 (ddd,  $J = 15.5, 9.6, 5.1$  Hz, 1H), 5.80 (s, 1H), 5.69 (dddd,  $J = 15.3, 7.3, 7.3, 1.5$  Hz, 1H), 5.50 (dd,  $J = 15.4, 4.8$  Hz, 1H), 5.49 (s, 1H), 5.38 (d,  $J = 1.0$  Hz, 1H), 5.36 (d,  $J = 1.0$  Hz, 1H), 5.21 (s, 1H), 4.88 (s, 1H), 4.79 (s, 1H), 4.72 (dd,  $J = 6.1, 3.2$  Hz, 1H), 4.59 (s br, 1H), 4.43 (s br, 1H), 4.22 (s br, 1H), 4.06 (t br,  $J = 3.8$  Hz, 1H), 3.21 (dd,  $J = 14.9, 5.0$  Hz, 1H), 3.11 (dd,  $J = 14.7, 9.3$  Hz, 1H), 2.85 (dd,  $J = 6.2, 2.2$  Hz, 1H), 2.76 (dd,  $J = 7.5, 2.2$  Hz, 1H), 2.76 (s br, 2H), 2.34 (dd,  $J = 15.3, 5.0$  Hz, 1H), 2.27 (d,  $J = 1.1$  Hz, 3H), 2.16 (m, 1H), 1.92 (dd,  $J = 14.4, 9.2$  Hz, 1H), 1.53–1.24 (m, 5H), 1.06 (d,  $J = 7.0$  Hz, 3H), 0.93 (d,  $J = 6.8$  Hz, 3H), 0.91 (t,  $J = 7.1$  Hz, 3H);  $^{13}\text{C}$  NMR (101 MHz,  $\text{CDCl}_3$ )  $\delta$  165.8, 152.8, 147.2, 145.0, 144.8, 136.4, 134.8, 130.9, 130.6, 118.6, 116.1, 114.7, 112.9, 75.8, 74.7, 73.5, 72.5, 70.5, 61.8, 54.2, 39.7, 39.0, 36.7, 36.2, 35.4, 33.3, 20.0, 15.8, 14.9, 14.3, 13.9. HRESIMS  $m/z$  calcd for  $\text{C}_{31}\text{H}_{46}\text{O}_7\text{Na}$  ( $\text{M}^+ + \text{Na}$ ) 553.3141, found 553.3157; optical rotation  $[\alpha]^{24}_{\text{D}} = +56$  (c 0.05,  $\text{CHCl}_3$ ).

**Acknowledgment.** We thank the National Institutes of Health (Grant GM-33049) for their generous support of our programs. J.D.C. and S.T.W. were supported by NIH postdoctoral fellow-

ships. Mass spectra were provided by the Mass Spectrometry Facility, University of San Francisco, supported by the NIH Division of Research Resources. We thank Professor Robert Maleczka, Professor Gerald Pattenden, and Dr. Lamont Terrell for sharing their spectral data for **1** and **36**. We also thank Professor Kobayashi for performing the comparison of **59** to natural amphidinolide A.

**Supporting Information Available:** Experimental procedures and characterization data for **9**, **10**, **12–16**, **29–31**, **43**, **45**, **49**, **51**, **53**, and **62**, and characterization data for **38–41**, **54**, **56**, **57**, and **59**. This material is available free of charge via the Internet at <http://pubs.acs.org>.

JA053365Y